

Mathematical modelling of combustion and biofuel co-firing in industrial steam generators

By

Michal BENEŠ¹ and Tomáš OBERHUBER² and Pavel STRACHOTA³ and
Robert STRAKA⁴ and Vladimír HAVLENA⁵

Abstract

In the contribution, we summarize results of mathematical modelling and numerical simulation of flow, transport, combustion and reaction processes in industrial steam generators powered by the powderized coal combustion with possible partial biofuel additives (biofuel co-firing). The model is based on numerical solution of conservation laws for mass, momentum, energy and composition of the most important components in combustion with respect to the energy release and to the carbon dioxide and nitrogen oxide release. Combustion process is described by means of the apriori knowledge of the coal-particle burn-out replacing the complex combustion chemistry. The undergoing chemical reactions are described by the Arrhenian kinetics. The energy transport includes radiative heat transfer approximated by the Rosseland model. The numerical approach is based on the finite-volume methods in combination with an advection upstream splitting method as the Riemann solver and with the Runge-Kutta time solver. Several computational results demonstrate the function of the model.

Received October 15, 2011. Revised June 13, 2012.

2000 Mathematics Subject Classification(s): 35M10, 35Q79, 76V05, 80A25, 65M08

Key Words: Navier-Stokes equations; multi-phase flow; combustion; turbulence; reactive flows.

The research is supported by the Research branch of ČVUT No. MSM 6840770010 *Applied Mathematics in Technical and Physical Sciences* and by the project *Advanced Control and Optimization of Biofuel Co-Firing in Energy Production* No. TA01020871 of the Technological Agency of the Czech Republic.

¹ Dept. of Mathematics, Faculty of Nuclear Sciences and Physical Engineering, Czech Technical University in Prague, Czech Republic.

e-mail: michal.benes@fjfi.cvut.cz

² Dept. of Mathematics, Faculty of Nuclear Sciences and Physical Engineering, Czech Technical University in Prague, Czech Republic.

e-mail: tomas.oberhuber@fjfi.cvut.cz

³ Dept. of Mathematics, Faculty of Nuclear Sciences and Physical Engineering, Czech Technical University in Prague, Czech Republic.

e-mail: pavel.strachota@fjfi.cvut.cz

⁴ Dept. of Heat Engineering and Environmental Protection, Faculty of Metal Engineering and Industrial Computer Science, AGH University of Science and Technology, Krakow, Poland.

e-mail: straka@sendzimir.metal.agh.edu.pl

⁵ Honeywell ACS AT Laboratory Prague, Czech Republic.

e-mail: vladimir.havlina@honeywell.com

§ 1. Introduction

The steam and electricity production worldwide is mostly provided by coal-based combustion devices. Their control with respect to optimal energy release and minimal pollution generation is of great and continuous interest of the producers. One of efficient ways to achieve an economically and environmentally reasonable compromise is using the model-based optimization and device control. For this purpose, an accurate and computationally efficient model of the combustion processes has to be developed which is incorporated into the control system afterwards.

This article summarizes the key parts of such a model related to a particular combustion facility design operating with the powdered coal with possible additives such as the biomass. The detailed description of the key physical and chemical processes allows to follow the operation levels of steam generation with respect to the fuel consumption, the CO_2 and nitrogen oxides production influenced by the fuel distribution over the burners.

Respecting the particular industrial design the combustion chamber is vertically positioned 30 m high 7 m wide, and has a square horizontal cross-section. At corners of the bottom part, the injection channels for the air and coal mixture and air are located. Additional air can be injected over the combustion kernel through the OFA (over-fire air) slots. The flue gas leaves the combustion chamber at the upper side and continues through the piping of heat exchangers. Schematics of this configuration can be seen in Figure 1. The flue-gas motion is forced by fans operating at the end of the flue gas channel. The average power production of the facility is about 90 MW and about 100 tons of the pressurized superheated steam per hour.

The operation of the described configuration is subject of frequent engineering studies - see e.g. [10, 13]. The current approach is gradually described in [3, 5, 6, 8]. The research on heat exchangers is summarized in [7].

§ 2. Mathematical model

The interest of the modelling is focused on the combustion chamber whose geometry including the injection slots is shown in Figure 2. The mathematical model is based on the balance laws for mass, component, momentum and energy conservation. The mixture of multiple components is used where the coal particles are treated as one of the phases. Unlike e.g. in [1], where the gas particles are treated separately and use separate equations of momentum, this approach simplifies the model when treating turbulence, and does not require several empirical relations and constants.

Currently, the following components of the mixture are considered:

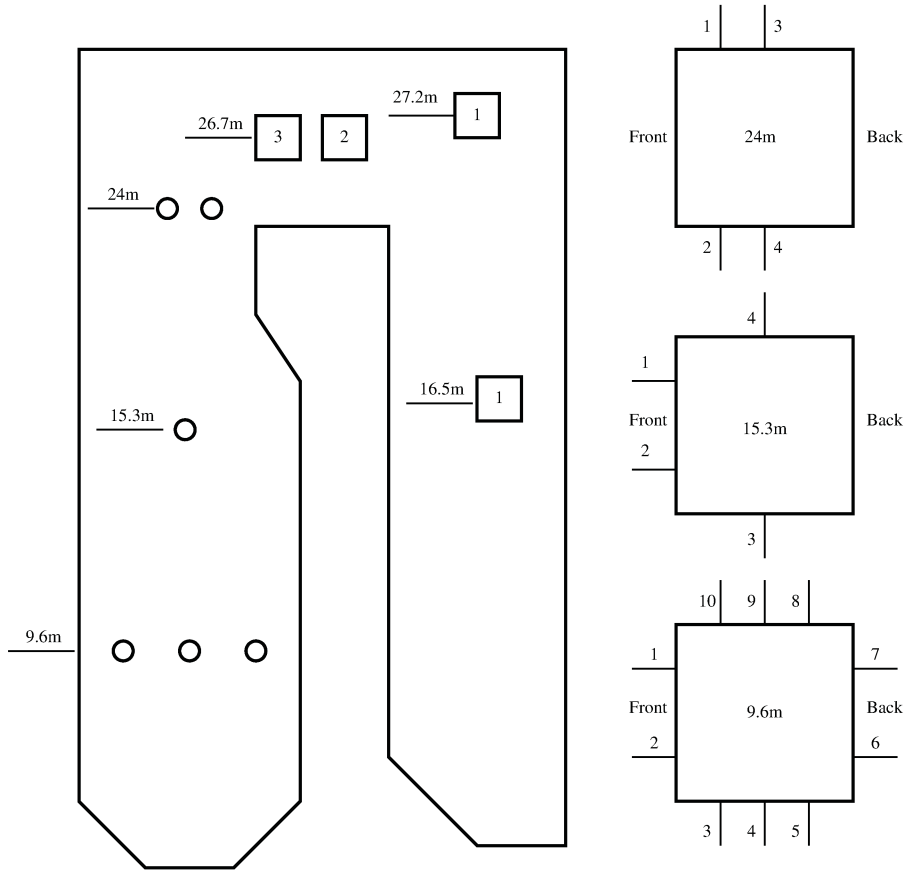


Figure 1. Overall configuration and measurement points

- chemical compounds engaged in major thermal and fuel NO_x reactions: nitrogen (N₂), oxygen (O₂), nitric oxide (NO), hydrogen cyanide (HCN), ammonia (NH₃), and water (H₂O)
- char and volatile part of the coal particles

The gas phase is described by the following equations. As stated above, the mass balance is described by equations of mass balance of each subcomponent (the Einstein summation is used)

$$(2.1) \quad \frac{\partial}{\partial t}(\rho Y_i) + \frac{\partial}{\partial x_j}(\rho Y_i u_j) = \nabla \vec{J}_i + R_i,$$

where ρ is the flue gas mass density, Y_i concentration of the component, and u_j are the gas velocity components. The right-hand side terms describe the laminar and turbulent diffusion of the components and either production or consumption due to chemical reactions within the R_i term.

The above equations of component mass balance are accompanied by the equation

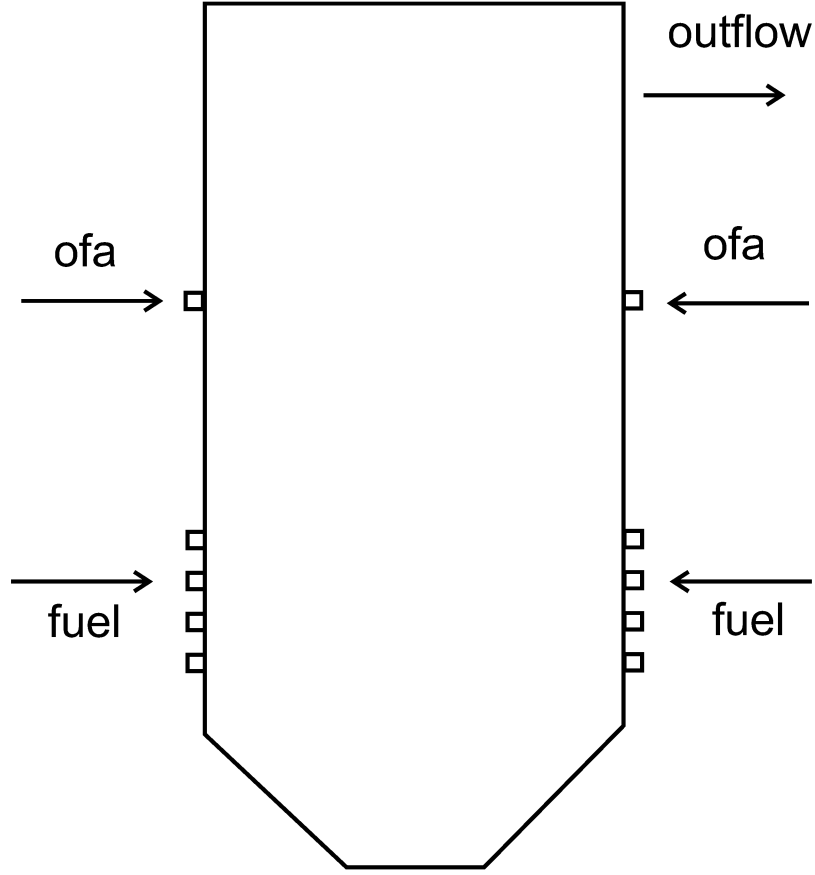


Figure 2. Geometrical configuration of the chamber.

of total mass balance

$$(2.2) \quad \frac{\partial \rho}{\partial t} + \frac{\partial(\rho u_j)}{\partial x_j} = 0.$$

Equations of momentum conservation are as follows

$$(2.3) \quad \frac{\partial}{\partial t}(\rho u_i) + \frac{\partial}{\partial x_j}(\rho u_i u_j) = -\frac{\partial p}{\partial x_i} + \frac{\partial}{\partial x_j} \left[\mu_{\text{eff}} \left(\frac{\partial u_i}{\partial x_j} + \frac{\partial u_j}{\partial x_i} - \frac{2}{3} \delta_{ij} \frac{\partial u_l}{\partial x_l} \right) \right] + g_i,$$

where $\vec{g} = [g_1, g_2, g_3]$ is the external force acting on the fluid, in our case the gravity. The effective friction coefficient μ_{eff} is calculated from the turbulence model as

$$\mu_{\text{eff}} = \mu + \mu_t = \mu + \rho C_\mu \frac{k^2}{\epsilon},$$

where μ is the laminar viscosity, k the turbulent kinetic energy, and ϵ the turbulent energy dissipation rate. Constant C_μ , like additional constants mentioned later in the description of the turbulence model, has to be chosen empirically for the particular problem, in our case we use $C_\mu = 0.09$, which seems to give satisfactory results.

The conservation of energy

$$(2.4) \quad \frac{\partial}{\partial t}(\rho h) + \frac{\partial}{\partial x_j}(\rho u_j h) = -n_{\text{coal}} \frac{dm_{\text{coal}}}{dt} h_{\text{comb}} + q_r + q_c + q_s,$$

has the right-hand side terms as the heat of combustion (h_{comb} as the specific enthalpy of combustion, n_{coal} the coal-particle density, m_{coal} the coal-particle mass), the heat transfer by radiation (q_r), heat transfer by conduction (q_c), and heat source or sink (q_s). The heat conduction is given by the Fourier law

$$q_c = -\nabla \cdot (\lambda \nabla T),$$

and

$$q_r = -\nabla \cdot (cT^3 \nabla T),$$

describes the transfer by radiation. The radiation heat transfer is fully described by an integral-differential equation of radiation, which is very computationally expensive to solve. However, as the flue gas can be considered an optically thick matter, the above approximation of the radiation flux called Rosseland radiation model can be applied [17].

The heat source term is nonzero only at the boundary and describes the energy exchange with the walls of the chamber via conduction and radiation

$$q_s = A(T_{\text{gas}} - T_{\text{wall}}) + B(T_{\text{gas}}^4 - T_{\text{wall}}^4),$$

where A and B are constants dependent on the properties of the interface between the modeled region and its surroundings.

The particle mass change rate is currently described by the one-step Arrhenian kinetics which is used separately for the char and volatile coal components — the combustion of the volatiles is faster than the combustion of the char

$$\frac{dm_p}{dt} = -A_v m_p^\alpha [\text{O}_2]^\beta \exp\left(-\frac{E_v}{RT_p}\right),$$

where m_p is the particle combustible mass, A_v , E_v are empirical constants, $[\text{O}_2]$ oxygen concentration and T_p is the particle temperature.

These equations are accompanied by the equation of state

$$p = (\kappa - 1) \rho_{\text{gas}} \left(e_{\text{gas}} - \frac{1}{2} u_i u_i \right).$$

Here, κ is the Poisson constant and e_{gas} is the gas energy per unit mass.

For the turbulence modeling, we use the standard k - ϵ model, which describes the evolution of turbulence using two equations — first one for turbulent kinetic energy

$$(2.5) \quad \frac{\partial}{\partial t}(\rho k) + \frac{\partial}{\partial x_j}(\rho k u_j) = \frac{\partial}{\partial x_j} \left[\left(\mu + \frac{\mu_t}{\sigma_k} \right) \frac{\partial k}{\partial x_j} \right] + G_k - \rho \epsilon,$$

and the second one for turbulent kinetic energy dissipation rate

$$(2.6) \quad \frac{\partial}{\partial t}(\rho\epsilon) + \frac{\partial}{\partial x_j}(\rho\epsilon u_j) = \frac{\partial}{\partial x_j} \left[\left(\mu + \frac{\mu_t}{\sigma_\epsilon} \right) \frac{\partial \epsilon}{\partial x_j} \right] + C_{1\epsilon} \frac{\epsilon}{k} G_k - C_{2\epsilon} \rho \frac{\epsilon^2}{k}.$$

Constants appearing in the turbulence model have to be determined empirically

The left-hand sides of the equations describe the passive advection of the respective quantities by the advection velocity \vec{u} . The right-hand sides describe their spatial diffusion, their production and dissipation.

The term G_k , which describes the production of turbulence, can be derived from the Reynolds averaging process and written in the terms of the fluctuating part of the velocity as

$$G_k = \tau_{jl} \frac{\partial u_j}{\partial x_l} = -\overline{\rho u'_j u'_l} \frac{\partial u_j}{\partial x_l},$$

where τ_{jl} is the Reynolds stress tensor. However during practical computation, the fluctuations u'_j and u'_l are unknown. Using the Boussinesq hypothesis, that the Reynolds stress is proportional to the mean strain rate

$$S_{ij} = \frac{1}{2} \left(\frac{\partial u_i}{\partial x_j} + \frac{\partial u_j}{\partial x_i} \right),$$

one can write turbulent production in closed form

$$G_k = \mu_t S^2, \quad S = (2S_{jl}S_{jl})^{1/2}.$$

The diffusion of the species consists of two processes — the laminar and turbulent one, and the diffusion term in equation (2.1) can be written in the form

$$\vec{J}_i = - \left(\rho D_{i,m} + \frac{\mu_t}{Sc_t} \right) \nabla Y_i.$$

The first term corresponds to linear laminar diffusion, the second one to turbulent diffusion. Given the fact that the turbulent diffusion generally predominates the Brownian one, and the term $D_{i,m}$ is difficult to determine, the Brownian diffusion can usually be ignored. The Sc_t coefficient is the turbulent Schmidt number.

The particle phase is evolved according to its balance law

$$(2.7) \quad \frac{\partial n_{\text{coal}}}{\partial t} + \frac{\partial (n_{\text{coal}} u_1)}{\partial x_1} + \frac{\partial (n_{\text{coal}} u_2)}{\partial x_2} = 0,$$

which allows to track the particle surface area important for the combustion process.

§ 3. Simplified model of NO_x chemistry

The model is designed to describe the amount of NO_x emissions leaving the combustion chamber. The mechanism of flue gas production in case of the coal combustion

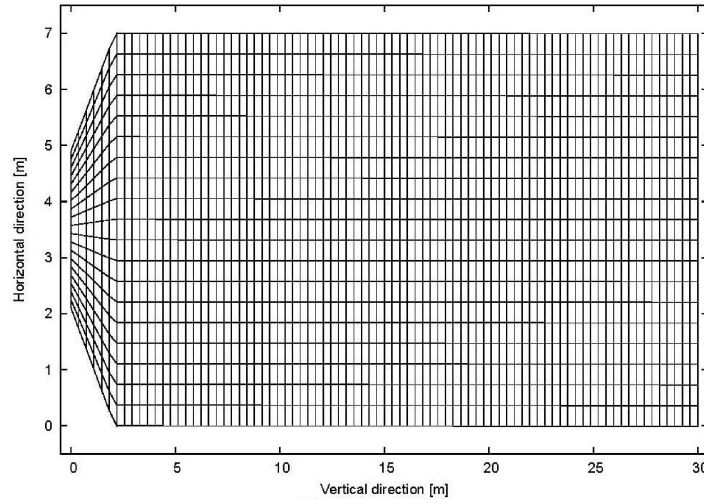


Figure 3. Finite-volume grid.

| Case | Air distribution % | | | | Fuel distribution % | | | | Excess air coefficient | | | |
|------|--------------------|-------|-------|-------|---------------------|-------|-------|-------|------------------------|-------|-------|-------|
| | B_1 | B_2 | B_3 | B_4 | B_1 | B_2 | B_3 | B_4 | B_1 | B_2 | B_3 | B_4 |
| 1 | 25 | 25 | 25 | 25 | 25 | 25 | 25 | 25 | 1.3 | 1.3 | 1.3 | 1.3 |
| 2 | 50 | 20 | 20 | 10 | 25 | 25 | 25 | 25 | 2.6 | 1.04 | 1.04 | 0.52 |
| 3 | 10 | 20 | 20 | 50 | 25 | 25 | 25 | 25 | 0.52 | 1.04 | 1.04 | 2.6 |
| 4 | 25 | 25 | 25 | 25 | 50 | 20 | 20 | 10 | 0.65 | 1.63 | 1.63 | 3.25 |

Table 1. Air-coal distributions.

seems to be complicated. Therefore, only the most important phenomena and reaction paths were considered in order to provide the maximum availability of such a model in the model-based real-time control engineering.

In most cases, NO_x is interpreted as the group of nitrogen oxide NO and nitrogen dioxide (NO_2), which strongly pollute our living environment. There are two major processes contributing to the total NO_x emission. The former is known as the *Thermal* NO_x or *Zeldovich* and simply consists of oxidation of the atmospheric nitrogen at high temperature conditions. The latter is called *Fuel* NO_x and describes the NO_x creation from nitrogen, which is chemically bonded in the coal fuel. The fuel NO_x usually is the major source of the NO_x emissions. These are the only mechanisms considered, although a few more could be involved (such as the *Prompt* NO_x (Fenimore) or the *Nitrous oxide* (N_2O) intermediate mechanisms).

The **thermal** NO generation mechanism is active at high temperature conditions (~ 1800 K) only, and is represented by a set of three equations, introduced by Zeldovich [9] and

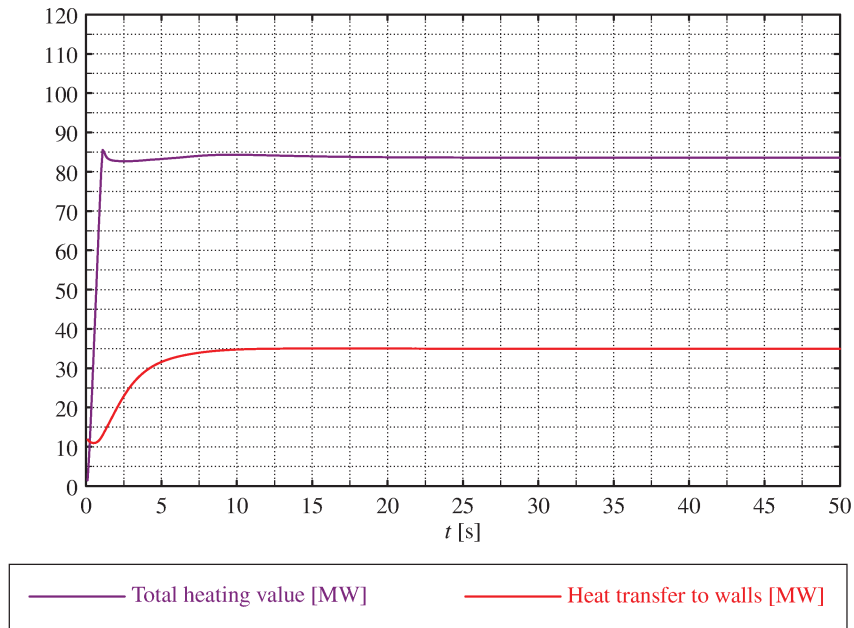


Figure 4. Time evolution of energy release and wall transfer.

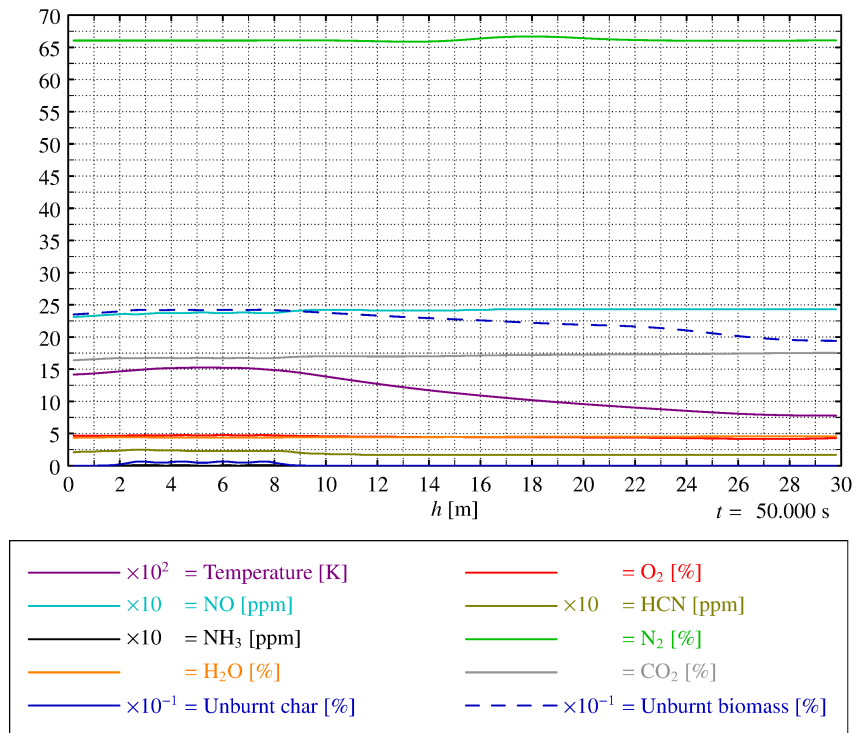
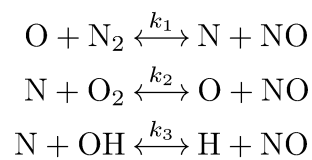


Figure 5. Vertical distribution of key system variables at a given time.

extended by Bowman [10]

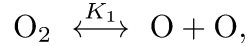


All these reactions are considered to be reversible. The rate constants can be found in [11].

In order to compute the NO concentration, concentrations of nitrogen radical [N], oxygen radical [O] and hydroxyl radical [OH] must be known. It is useful to assume [N] to be in a quasi-steady state according to its nearly immediate conservation after creation. In fact, this N-radical formation is the rate limiting factor for thermal NO production, due to an extremely high activation energy of nitrogen molecule, which is caused by a triple bond between two nitrogen atoms. Hence, NO formation rate can be stated as

$$\frac{d[\text{NO}]}{dt} = 2k_1^+ \cdot [\text{O}] \cdot [\text{N}_2] \cdot \frac{1 - \frac{k_1^- k_2^- [\text{NO}]^2}{k_1^+ [\text{N}_2] k_2^+ [\text{O}_2]}}{1 + \frac{k_1^- [\text{NO}]}{k_2^+ [\text{O}_2] + k_3^+ [\text{OH}]}}.$$

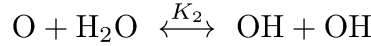
Under certain conditions, oxygen molecule splits and recombines cyclically



which can be profitably described by following partial equilibrium approach

$$[\text{O}] = K_1 \cdot [\text{O}_2]^{1/2} \cdot T^{1/2}.$$

As for OH radical, a similar partial equilibrium approach can be taken. According to the reaction



we obtain

$$[\text{OH}] = K_2 \cdot [\text{O}]^{1/2} \cdot [\text{H}_2\text{O}]^{1/2} \cdot T^{-0.57}.$$

The factors $K_1 = K_1(T)$ and $K_2 = K_2(T)$ are expressed as follows

$$K_1 = 36.64 \cdot \exp\left(\frac{-27123}{T}\right),$$

$$K_2 = 2.129 \cdot 10^2 \cdot \exp\left(\frac{-4595}{T}\right).$$

Fuel NO. Composition analysis shows, that nitrogen-based species are more or less present in coal, usually as mass fractions of 0.1 % to 1 %. When the coal is heated, these species are transformed into certain intermediates and then into NO. Fuel itself is therefore a significant source of NO pollutants. When a coal particle is heated, it is presumed that nitrogen compounds are distributed into volatiles and char. Some studies (e.g. [12]) claim that one half the nitrogen converts into volatiles and second half into char. Since there is no reason for such an assumption, a parameter α is introduced to describe the distribution

$$m_{\text{vol}}^{\text{N}} = \alpha \cdot m_{\text{tot}}^{\text{N}},$$

$$m_{\text{char}}^{\text{N}} = (1 - \alpha) \cdot m_{\text{tot}}^{\text{N}},$$

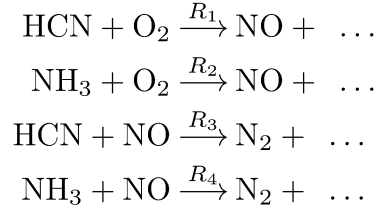
where $\alpha \in \langle 0, 1 \rangle$, $m_{\text{tot}}^{\text{N}}$ is the total mass of nitrogen, $m_{\text{vol}}^{\text{N}}$ is the mass of nitrogen in volatiles and $m_{\text{char}}^{\text{N}}$ is the mass of nitrogen in char.

As already mentioned, nitrogen transforms to pollutants via intermediates, which usually are ammonia NH_3 and hydrocyanide HCN . For further proceeding, we must define four parameters to describe complex partitioning of the fuel bound nitrogen.

- β is amount of volatile bounded nitrogen which converts to HCN .
- δ_1 is distribution of char bounded nitrogen which converts to HCN .
- δ_2 is distribution of char bounded nitrogen which converts to NH_3 .
- δ_3 is distribution of char bounded nitrogen which converts to NO .
- $\beta \in \langle 0, 1 \rangle$, $\delta_1 + \delta_2 + \delta_3 = 1$.

Different parametric studies should be carried out to find the best values of α , β , δ_1 , δ_2 and δ_3 suitable for specific type of coal. Five overall reactions of either NO formation or depletion were incorporated in the combustion part of the numerical code.

NO, HCN, NH_3 reactions. According to [15], formation rates of reactions

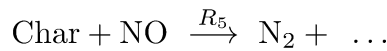


are given as

$$\begin{aligned} R_1 &= 1.0 \cdot 10^{10} \cdot X_{\text{HCN}} \cdot X_{\text{O}_2}^a \cdot \exp\left(\frac{-33732.5}{T}\right), \\ R_2 &= 4.0 \cdot 10^6 \cdot X_{\text{NH}_3} \cdot X_{\text{O}_2}^a \cdot \exp\left(\frac{-16111.0}{T}\right), \\ R_3 &= -3.0 \cdot 10^{12} \cdot X_{\text{HCN}} \cdot X_{\text{NO}} \cdot \exp\left(\frac{-30208.2}{T}\right), \\ R_4 &= -1.8 \cdot 10^8 \cdot X_{\text{NH}_3} \cdot X_{\text{NO}} \cdot \exp\left(\frac{-13593.7}{T}\right), \end{aligned}$$

where X is the mole fraction and a is the oxygen reaction order.

Heterogeneous NO reduction on char. Present char allows following adsorption process to occur



Levy [16] uses pore surface area (BET) to define NO source term

$$S_{\text{ads}}^{\text{NO}} = k_5 \cdot c_s \cdot A_{\text{BET}} \cdot M_{\text{NO}} \cdot p_{\text{NO}},$$

where $k_5 = 2.27 \cdot 10^{-3} \cdot \exp\left(\frac{-17168.33}{T}\right)$ is the rate constant, $S_{\text{ads}}^{\text{NO}}$ is the NO source term, c_s is the concentration of particles, A_{BET} is the pore surface area and p_{NO} is the partial pressure of NO.

In order to evaluate overall NO source term, single source terms have to be summarized. This overall source term can be further used in transport equations. As for HCN and NH_3 source terms, it is possible to determine them from coal burnout rate. It is assumed, that nitrogen from both char and volatiles transforms to intermediate species quickly and totally.

Algebraic Unified Second-Order Moment reaction model. The complexity of chemical reactions leading to the NO_x formation during combustion and turbulent flow requires a careful treatment of the reaction model for each reaction. The approach described in [18, 19] can be applied as shown in [6]. Consider one of the above mentioned two-component second-order reactions for which the Arrhenius kinetics is described by the instantaneous reaction rate

$$w_s = A \varrho^2 Y_1 Y_2 k(T),$$

where A is the pre-exponential factor, Y_1, Y_2 are instantaneous species mass fractions, $k(T) = \exp(-E/RT)$ is the reaction-rate coefficient, E is the activation energy, and R is the universal gas constant. When performing the Reynolds expansion and time averaging, and neglecting the third-order correlation, the time-averaged reaction rate is obtained as

$$\overline{w_s} = A \varrho^2 \left[\left(\overline{Y_1 Y_2} + \overline{Y_1' Y_2'} \right) \bar{k} + \overline{Y_1 k' Y_2'} + \overline{Y_2 k' Y_1'} \right].$$

Special attention is paid to the highly nonlinear coefficient $k(T)$ with difficult behavior during turbulent combustion. We express

$$\bar{k} = \int \exp\left(-\frac{E}{RT}\right) P(T) dT$$

as the time-averaged value by means of the probability-density distribution function $P(T)$ depending on temperature. The second-order moments $\overline{Y_1' Y_2'}$, $\overline{k' Y_1'}$, $\overline{k' Y_2'}$ are evaluated by means of their evolution transport averaged equations. The solution of such equations can be simplified by neglecting the convection and diffusion of these quantities. The resulting expressions have algebraic form

$$\overline{Y_1' Y_2'} = C_{12} \frac{\partial \bar{Y}_1}{\partial x_j} \frac{\partial \bar{Y}_2}{\partial x_j}, \quad \overline{k' Y_1'} = C_{k1} \frac{\partial \bar{k}}{\partial x_j} \frac{\partial \bar{Y}_1}{\partial x_j}, \quad \overline{k' Y_2'} = C_{k2} \frac{\partial \bar{k}}{\partial x_j} \frac{\partial \bar{Y}_2}{\partial x_j},$$

where the expressions C_{12} , C_{k1} , C_{k2} are given by the form of the averaged transport equations for the second-order moments.

§ 4. Biomass additives

Current energy production is influenced by the efforts of using renewable resources. As a consequence, simultaneous combustion of coal and biomass became frequent. Technologically, it brings new challenges as the additives though being renewable have rather different properties and lower energy content. In our case, the biomass pellets are considered as the additive. They have twice as less energy to be obtained by combustion, less water and ashes, half of carbon content. On the other hand, the pellets as well as the coal pieces are milled into the same powder geometry. Therefore, the model of combustion using the burnout process similar to coal particles can be used.

§ 5. Numerical algorithm

For numerical solution of the equations, finite volume method is used. For left and right hand sides in Eqs. (2.1), (2.2), (2.3), (2.4), (2.5), (2.6), (2.7), advection upstream splitting method (see [2]) is used to approximate fluxes in the FVM formulation, and edge dual-volume approximation is used to approximate the second order derivatives respectively. The discretization is performed on a structured grid as shown in Figure 3. For detailed description of the solution procedure see [5, 6].

§ 6. Simulation results

In this section, a series of computational results is presented showing the qualitative behaviour of the model under different model settings. First, a study distinguishing the behaviour for different distributions of the coal and air in four burners is presented.

- **Case 1** - uniform air and coal distribution over 4 pairs of burners
- **Case 2** - decreasing air and uniform coal distribution over 4 pairs of burners (with consequent excess or missing air fraction in burners)
- **Case 3** - increasing air and uniform coal distribution over 4 pairs of burners (with consequent excess or missing air fraction in burners)
- **Case 4** - uniform air and decreasing coal distribution over 4 pairs of burners (with consequent excess or missing air fraction in burners)

The setting is shown in Table 1. Corresponding results are shown in Figures 6-9.

A sample of biomass co-firing is shown in Figure 4 with the heat transfer data, and in Figure 5 with the profiles of relevant system quantities along the main geometry axis.

§ 7. Conclusion

The article briefly describes main aspects of the mathematical and numerical model of the pulverized-coal combustion. The model has been developed using a simplifying idea of the a-priori knowledge of the fuel-particle burnout properties. The computational results show the qualitative behaviour of the model. The obtained results have been compared with the real measurements at point indicated in Figure 2 providing a satisfactory agreement. Future development will be focused on the studies of the influence of the over-fire slots and development of the model in the full 3D geometry.

References

- [1] Guo, Y.C., Chan, C.K., A Multi-Fluid Model for Simulating turbulent Gas-particle Flow and Pulverized Coal Combustion, *Fuel* 79 (12) (2000) pp. 1467-1476.
- [2] Liou, M.S., Steffen Jr., C., A New Flux Splitting Scheme, *J. Comp. Phys.* 107 (1) (1993) pp. 23-29.
- [3] Makovička, J., Havlena, V., Finite Volume Numerical Model of Coal Combustion, in: Beneš, M., Mikyška, J., Oberhuber, T. (Eds.), *Proceedings of the Czech-Japanese Seminar in Applied Mathematics 2004*, Faculty of Nuclear Sciences and Physical Engineering, Czech Technical University in Prague, (2005), pp. 106-116.
- [4] Makovička, J., Havlena, V. and Beneš M., On a model of coal combustion, in ALGORITHMY 2005, peer reviewed Proceedings of contributed papers and posters, pp. 12–21, Publ. house of STU (2005)
- [5] Makovička, J., Beneš, M., Havlena, V., Model of Turbulent Coal Combustion, *Proceedings of the Czech-Japanese Seminar in Applied Mathematics 2005*, Kuju Training Center, Oita, Japan, (2006), pp. 95-105.
- [6] Straka, R., Makovička, J., *Model of pulverized coal combustion in furnace*. Kybernetika Vol. 43 (2007), No. 6, 879–891.
- [7] Makovička, J., Havlena, V., Beneš, M., Mathematical modelling of steam and flue gas flow in a heat exchanger of a steam boiler, in: Handlovičová, A., Krivá, Z., Mikula, K., Ševčovič, D. (Eds.), *ALGORITHMY 2002 Proceedings of contributed papers*, Publ. house of STU, (2002), p. 171–178.
- [8] Straka R., Makovička J. and Beneš M. Numerical model of air-staging and OFA in PC boiler, in Algorithmy 2009, Proceedings of contributed papers and posters, ed. Handlovičová A., Frolkovič P., Mikula K. and Ševčovič D. Slovak University of Technology in Bratislava, Publishing House of STU, 2009
- [9] Zeldovich, J.B., The Oxidation of Nitrogen in Combustion and Explosions, *Acta Physicochimica* 21 (1946) pp. 577-628.
- [10] Bowman, C.T., Seery, D.J., *Emissions from Continuous Combustion Systems*, Plenum Press, New York, (1972), p. 123.
- [11] NIST, *Chemical Kinetics Database on the Web*, National Institute of Standards and Technology, (2000), <http://www.kinetics.nist.gov>
- [12] Kim, C., Lior, N., A numerical analysis of NO_x formation and control in radiatively/conductively-stabilized pulverized coal combustors, *Chemical Engineering Journal* 71 (3) (1998) pp. 221-231.

- [13] Smoot, L.D., Smith, P.J., *Coal Combustion and Gasification*, Plenum Press, New York, (1985), p. 373.
- [14] Lockwood, F.C., Romo-Millares, C.A., Mathematical Modeling of Fuel-NO Emissions from PF. Burners, *J. Inst. Energy* 65 (1992) pp. 144-152.
- [15] De Soete, G.G., Overall Reaction Rates of NO and N₂ Formation from Fuel Nitrogen, *Proc. Combust. Inst.* 15 (1975) pp. 1093-1102.
- [16] Levy, J.M., Chen, L.K., Sarofim, A.F., Beer, J.M., NO/Char reactions at pulverized coal flame conditions, *Proc. Combust. Inst.* 18 (1981) pp. 111-120.
- [17] FLUENT Inc., *FLUENT user's guide*, (2005).
- [18] Zhou, L.X., Zhang, Y., Zhang, J., *Simulation of swirling coal combustion using a full two-fluid model and an AUSM turbulence-chemistry model*, *Fuel* 82, (2003), pp. 1001-1007.
- [19] Zhou, L.X., *Development of SOM combustion model for Reynolds-averaged and large-eddy simulation of turbulent combustion and its validation by DNS*, *Science in China Series E: Technological Sciences* (2008), Vol. 51 No. 8, 1073-1086.

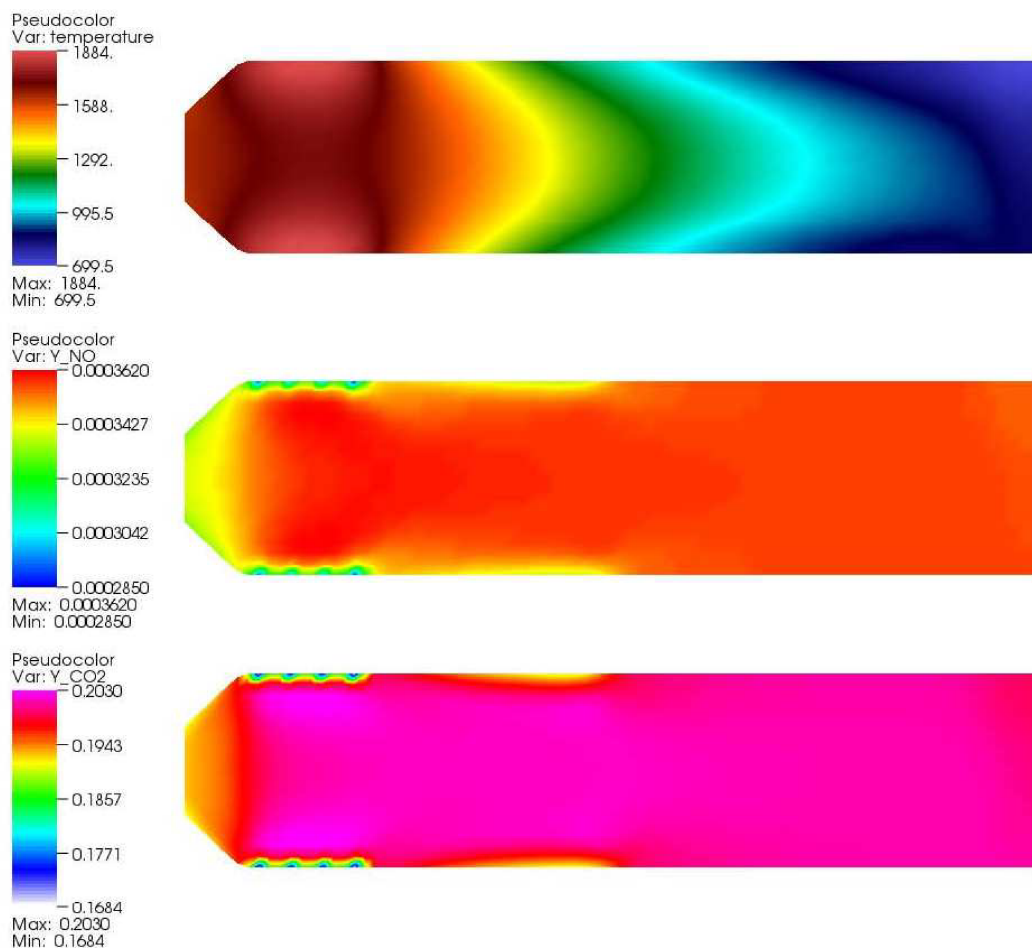


Figure 6. **Case 1:** Profiles of temperature (top), mass fraction of NO (middle) and mass fraction of CO₂ (bottom)

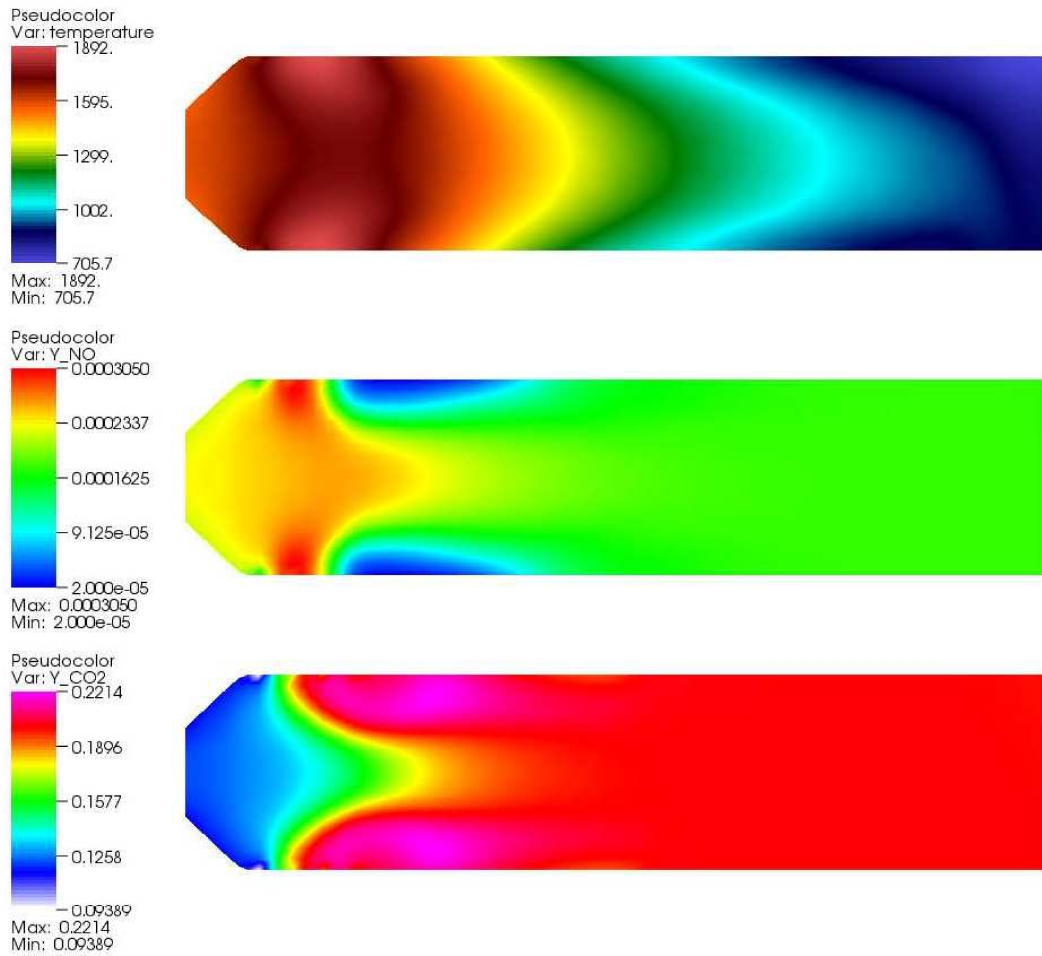


Figure 7. **Case 2:** Profiles of temperature (top), mass fraction of NO (middle) and mass fraction of CO₂ (bottom)

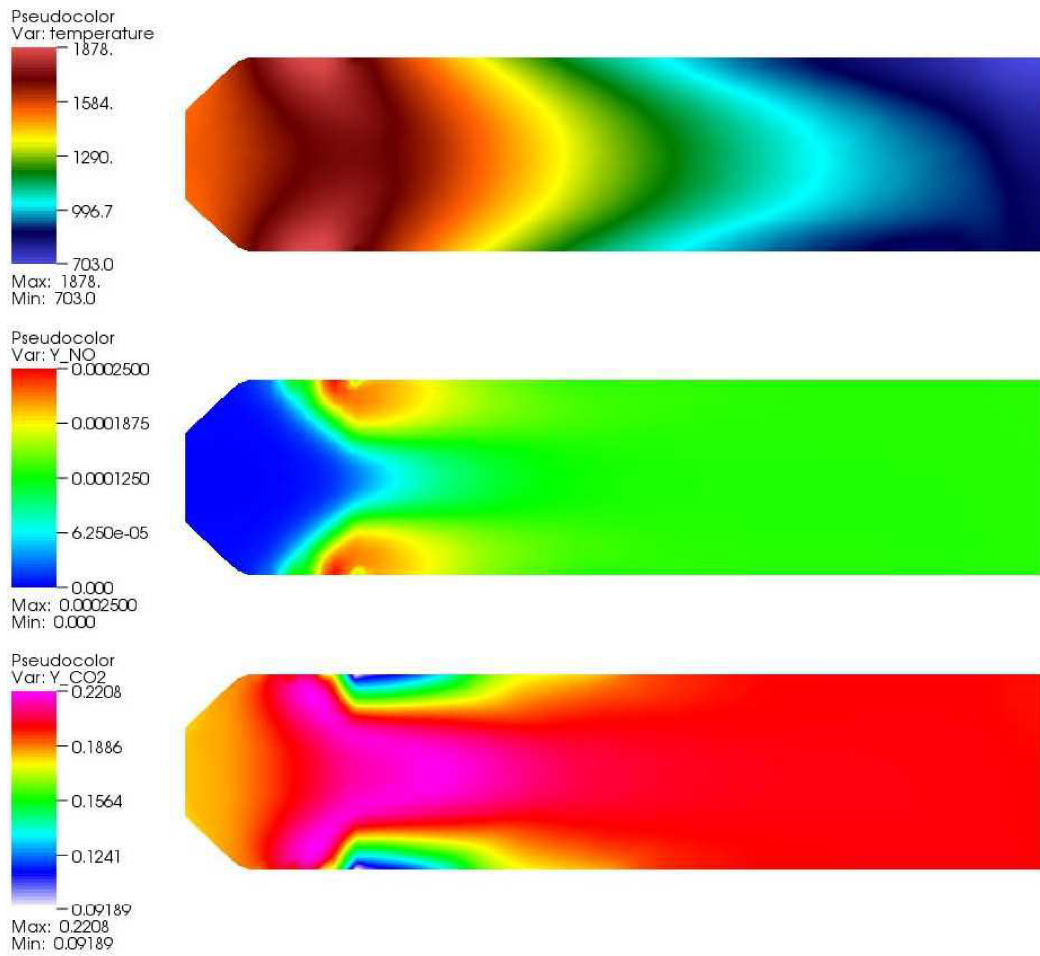


Figure 8. **Case 3:** Profiles of temperature (top), mass fraction of NO (middle) and mass fraction of CO₂ (bottom)

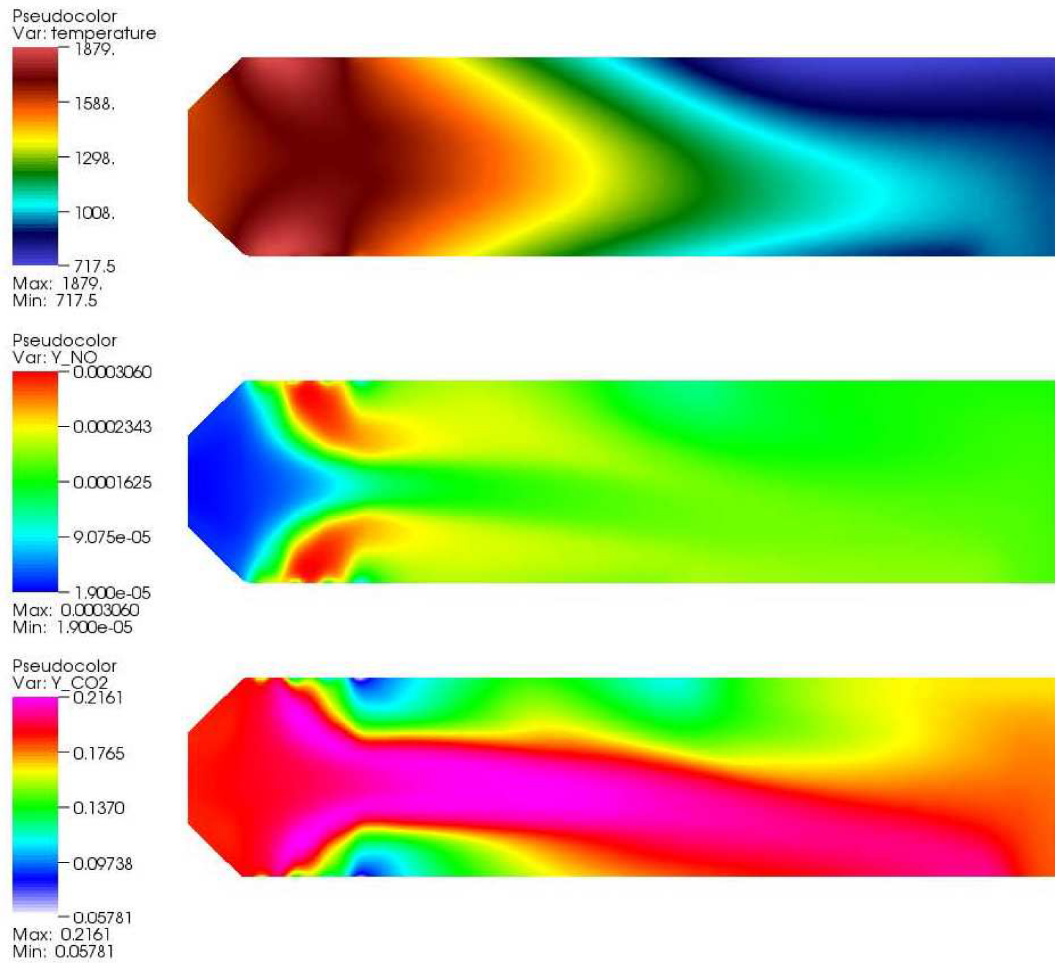


Figure 9. **Case 4:** Profiles of temperature (top), mass fraction of NO (middle) and mass fraction of CO₂ (bottom)